

Study of Ammonium Sulfide Surface Treatment for Ultrathin  
Cu(In,Ga)Se<sub>2</sub> with Different Cu/(Ga plus In) Ratios

Peer-reviewed author version

BULDU KOHL, Dilara; DE WILD, Jessica; KOHL, Thierry; BRAMMERTZ, Guy;  
BIRANT, Gizem; MEURIS, Marc; POORTMANS, Jef & VERMANG, Bart (2020)  
Study of Ammonium Sulfide Surface Treatment for Ultrathin Cu(In,Ga)Se<sub>2</sub> with  
Different Cu/(Ga plus In) Ratios. In: PHYSICA STATUS SOLIDI A-APPLICATIONS  
AND MATERIALS SCIENCE, 217 (19) (Art N° 2000307).

DOI: 10.1002/pssa.202000307

Handle: <http://hdl.handle.net/1942/32930>

1 **Study of ammonia sulfide surface treatment for ultra-thin Cu(In,Ga)Se<sub>2</sub> with different**  
2 **Cu/(Ga+In) ratios**

3  
4 *Dilara Gokcen Buldu\**, Jessica de Wild, Thierry Kohl, Guy Brammertz, Gizem Birant, Marc  
5 Meuris, Jef Poortmans, Bart Vermang

6  
7 ((Optional Dedication))  
8

9 D. G. Buldu, J. de Wild, T. Kohl, Prof. G. Brammertz, G. Birant, Dr. M. Meuris, Prof. J.  
10 Poortmans, Prof. B. Vermang  
11 Institute for Material Research (IMO), Hasselt University (partner in Solliance), Agoralaan  
12 gebouw H, Diepenbeek, 3590, Belgium  
13 E-mail: Dilara.Gokcen.Buldu@imec.be  
14 dilara.buldu@uhasselt.be  
15

16 D. G. Buldu, J. de Wild, T. Kohl, Prof. G. Brammertz, G. Birant, Dr. M. Meuris, Prof. B.  
17 Vermang  
18 Imec division IMOMECEC (partner in Solliance), Wetenschapspark 1, 3590 Diepenbeek,  
19 Belgium  
20

21 D. G. Buldu, J. de Wild, T. Kohl, Prof. G. Brammertz, G. Birant, Dr. M. Meuris, Prof. J.  
22 Poortmans, Prof. B. Vermang  
23 EnergyVille, Thorpark, Poort Genk 8310 & 8320, 3600, Belgium  
24

25 Prof. J. Poortmans  
26 imec (partner in Solliance), Kapeldreef 75, Leuven, 3001, Belgium  
27

28 Prof. J. Poortmans  
29 Department of Electrical Engineering, KU Leuven, Kasteelpark Arenberg 10, 3001 Heverlee,  
30 Belgium  
31

32  
33 Keywords: surface treatment, Cu(In,Ga)Se<sub>2</sub>, CGI ratio, thin film photovoltaics,  
34 photoluminescence  
35

36 In ultra-thin Cu(In,Ga)Se<sub>2</sub> (CIGS) film solar cells, the CdS/CIGS interface may become one  
37 of the limiting factors for efficiency. The first step towards reducing the impact of this  
38 problem could be a surface treatment process to improve the quality of the front interface. The  
39 purpose of this study is to have a better understanding of the effect of wet chemical surface  
40 treatment, using ammonium sulfide ((NH<sub>4</sub>)<sub>2</sub>S), on CIGS thin film layers with different  
41 Cu/(Ga+In) (CGI) ratios. Photoluminescence (PL) and time-resolved PL (TRPL) studies were  
42 carried out on bare CIGS, ammonium sulfide treated CIGS thin films, and samples with CdS.  
43 In bare CIGS, CGI ratio dependent changes in PL were observed both on a low energy (defect

1 related transition) and a high energy peak (band to band transition). After the surface  
2 treatment, PL maximum increases by factors ranging from 4 to 11 depending on CGI ratio,  
3 accompanied by a slower decay. Trends with similar improvement as in the PL study were  
4 observed in the performance of the solar cells. We showed that the impact of the surface  
5 treatment is beneficial independently of the CGI ratio of the absorber layers. In all cases, the  
6 treatment was shown to improve the efficiency.

## 7 8 **1. Introduction**

9 Among all thin film photovoltaic technologies (PV), CIGS thin film is one of the most studied  
10 materials due to its high conversion efficiencies, beyond 23%.<sup>[1]</sup>In addition to its high  
11 efficiencies, it has high potential for application in building-integrated PV solutions, which  
12 makes it an interesting candidate for the new emerging applications on the market.  
13 Nevertheless, CIGS is still far away from becoming dominant on the photovoltaic market. For  
14 CIGS thin film PV to compete with dominant Si-PV technologies, its production costs will  
15 have to be reduced. One of the ways to reduce production costs is to reduce the thickness of  
16 CIGS material and, consequently, limit the usage of scarce elements such as In and Ga.  
17 Another way is to use a simple and energy efficient deposition method such as one-stage co-  
18 evaporation to deposit the CIGS layers. Because of the one-stage process, there will be no Ga  
19 gradient which will also improve the repeatability of the process. Yet, in the absence of a Ga  
20 gradient at the rear surface, when reducing the thickness of the absorber layer, interface  
21 recombination may become one of the factors limiting the performance of the solar cells. In  
22 addition, when there is no Ga-grading towards the front surface, the recombination increases  
23 at the buffer/CIGS interface, and thus, open circuit voltage can be decreased.<sup>[2]</sup>Hence,  
24 implementing a passivation layer at front and rear interfaces becomes important to overcome  
25 the impact of this limitation. There have been successful studies for rear surface  
26 passivation.<sup>[3,4]</sup>More recently, new studies have investigated the front surface

1 passivation.<sup>[5,6]</sup>The first study was based on a metal-insulator-semiconductor device structure  
2 where a very thin gallium oxide ( $\text{GaO}_x$ ) layer was used as a passivation layer. This study  
3 showed that the efficiency of the solar cells improved with a very thin (less than 2nm)  
4 passivation layer.<sup>[5]</sup>Furthermore, the first implementation of a passivation layer with openings  
5 on the front interface of CIGS was recently demonstrated. However, no significant  
6 improvements to efficiency and open-circuit potential ( $V_{oc}$ ) were observed.<sup>[6]</sup>As can be seen,  
7 the front surface passivation of CIGS absorbers is still challenging. In other words, the  
8 expected improvement has not yet been achieved. The surface properties of the absorber such  
9 as surface roughness, the most common copper selenide secondary phases, and impurities at  
10 the surface can be a critical factor. For that reason, the CIGS surface must be as clean as  
11 possible before further processing steps.

12 Several studies have reported that wet-chemical surface treatments before the CdS buffer  
13 layer deposition are a way to improve the efficiency of CIGS solar cells. Surface treatments  
14 lead to improved surface properties by removing secondary phases and undesired oxides,  
15 and/or passivating the surface. Most commonly, a KCN treatment is used to etch  $\text{Cu}_{2-x}\text{Se}$   
16 secondary phase on Cu-rich CIGS thin films.<sup>[7,8]</sup>However, KCN is highly toxic, which is why  
17 recently ammonium sulfide has been investigated as an alternative and safer solution to  
18 KCN.<sup>[9]</sup>Also,  $\text{NH}_3$  treatment is well-known for eliminating any oxides present on the  
19 surface.<sup>[10,11]</sup>However, despite the apparent advantages of this surface treatment, possible  
20 disadvantages also have to be taken into account. For example, by etching In and Ga, the  $\text{NH}_3$   
21 treatment promotes the creation of a Cu-Se layer and interface defects may be created by  
22 using highly concentrated  $\text{NH}_3$  solutions.<sup>[11,12]</sup>Beside these treatments, surface sulfurization is  
23 also used to improve the performance of solar cells. Nakada et al. used an aqueous solution  
24 for surface sulfurization and reported that cell performance is improved either through the  
25 formation of a very thin sulfide layer, or because the surface is passivated by sulfur  
26 atoms.<sup>[13]</sup>Another study showed that sulfurization with an  $\text{Na}_2\text{S}$  and thiourea solution can

1 replace the surface oxides by sulfides. The  $O_{Se}$  acceptor type defect is replaced with a  $S_{Se}$   
 2 because of the smaller electronegativity difference between In and S. This substitution may be  
 3 more efficient to decrease surface recombination.<sup>[14]</sup>In light of the reported studies, finding  
 4 optimal parameters of the surface treatments and a suitable surface treatment plays a key role  
 5 in improving the efficiency of CIGS solar cells.

6

## 7 **2. Result and Discussion**

### 8 **2.1. The effect of Cu/(Ga+In) ratio on the photoluminescence of bare CIGS thin films**

9 Three different types of CIGS films were used in this part. These samples are named  
 10 according to their CGI ratio. Samples with different CGI ratios of 0.72 (Cu-poor), 0.8 (Cu-  
 11 desired) and 0.92 (Cu-rich) were prepared to investigate the effect of CGI ratio. The PL  
 12 spectra of the as prepared absorber layer as well as their calculated energy bandgap value and  
 13 their peak maximum (dashed line) for each CGI ratio are given in **Figure 1**. The bandgap was  
 14 calculated using the following equation<sup>[15]</sup>:

$$15 \quad E_g(x) = E_g^{CGS}(x) + E_g^{CIS}(1 - x) - bx(1 - x)(1)$$

16 where x is the GGI ratio,  $E_g^{CGS}=1.68\text{eV}$  is the band gap of  $\text{CuGaSe}_2$  and  $E_g^{CIS}=1.02\text{eV}$  that of  
 17  $\text{CuInSe}_2$ . The bowing parameter b is 0.21eV. The GGI ratios are  $x=0.31$  and  $x=0.34$  for Cu-  
 18 poor and Cu-rich samples, respectively, and  $x=0.27$  for the Cu-desired sample. As can be seen  
 19 in Figure 1, two peaks appear in the PL spectra one at high- and one at low energy. While the  
 20 peak positions depend on the GGI, the ratio between the low and higher energy peak change  
 21 with the CGI ratio, similar to what we observed before.<sup>[16]</sup>The peak at high energy can be  
 22 identified as band to band transition. With increasing CGI ratio, both the PL peak maximum  
 23 and its full width at half maximum (FWHM) decrease. One possible reason for this effect  
 24 could be a reduced presence of copper vacancies with increasing CGI ratio.<sup>[17]</sup>On the other  
 25 hand, the low energy peak, which is clearly visible in Cu-desired and Cu-rich samples, could  
 26 be related to a defect. For the Cu-poor sample, a significant energy shift can be observed

1 compared to the calculated bandgap, implying the peak is mainly due to a very intense defect  
2 related transition. The band to band transition peak merges with the defect peak, thus forming  
3 the broad peak one can see on **Figure 1**. In their study, Hultqvist et al. showed, by using  
4 different buffer layers, that similar PL spectra contain a low, medium and high energy  
5 peak.<sup>[18]</sup> They suggested that these extra peaks below the band gap, could not be related to the  
6 absorber alone, but interface defects as well. In our case, we can tell that this low energy peak  
7 is not due to the CIGS/CdS buffer layer interface since we investigated the bare CIGS  
8 absorber (Figure 1). Instead, we think that the low energy peak is related to the copper  
9 vacancies as well, since its PL peak maximum and FWHM show changes with CGI. The Cu-  
10 poor samples with a CGI ratio of 0.72, has a 21 at.% Cu concentration. Cu-desired and Cu-  
11 rich are grown with a CGI ratio of 0.8 (22.5 at.% Cu) and 0.92 (24.5 at.%) respectively. When  
12 examining the phase diagram of  $\text{CI(G)Se}$ , it can be seen that between 16 at.% and 24 at.% Cu  
13 content, the material has two phases which are  $\text{CuIn(Ga)Se}_2$  and an ordered defect compound  
14 (ODC). This ODC defect consists of a Cu vacancy ( $V_{\text{Cu}}$ ) and an antisite defect of In on Cu  
15 ( $\text{In}_{\text{Cu}}$ ). The  $V_{\text{Cu}}$  acceptor and  $\text{In}_{\text{Cu}}^{2+}$  donor defects easily form a neutral defect pair ( $2V_{\text{Cu}}+$   
16  $\text{In}_{\text{Cu}}$ ).<sup>[13,14]</sup> This complex defect ( $2V_{\text{Cu}}+\text{In}_{\text{Cu}}$ ) is expected to be electrically inactive.<sup>[15,19,20]</sup> In  
17 the Cu-desired sample, the low energy peak was observed at around 1.04 eV which is 110  
18 meV lower than the band to band transition (1.15eV). This peak cannot be related only to an  
19 isolated  $V_{\text{Cu}}$  defect because the acceptor-type defect level of  $V_{\text{Cu}}$  is reported to be 30  
20 meV.<sup>[21,22]</sup> Since the peak at low energy is significantly deeper than this, it could be related to  
21 a defect complex that includes  $V_{\text{Cu}}$ . We propose that this defect could be related either to the  
22 neutral complex defect ( $2V_{\text{Cu}}+\text{In}_{\text{Cu}}$ ) or the acceptor type defect  $\text{O}_{\text{Se}}$ , since the difference in  
23 the position of the PL peaks matches the reported energies for these defects.<sup>[23-26]</sup> However,  
24 Ishizuka et. al show that the behavior of the acceptor  $\text{O}_{\text{Se}}$  defect changes with sodium  
25 incorporation.<sup>[26]</sup> Thus, this defect cannot be the defect that we observed at low energy, since  
26 our samples have all been supplied with the same amount of sodium. Due to this, we conclude

1 that the observed peak at low energy is most probably related to the neutral complex defect  
2 ( $2V_{Cu} + In_{Cu}$ ).

### 3 **2.2. The effect of ammonium sulfide (AS) surface treatment on the photoluminescence of** 4 **CIGS thin films**

5 In this section, we study the evolution of PL and TRPL responses of our samples after each of  
6 the processing steps. For each CGI ratio we created a set of two absorbers: i- standard process  
7 (bare CIGS - CdS) referred to as w/o AS, ii- surface treatment process (bare CIGS - AS  
8 treatment -CdS) referred to as w/AS. Firstly, the bare CIGS samples for each set were  
9 measured. Then, the measurements were performed after AS (for the AS-treated absorber of  
10 each set) and after CdS (for both samples in each sets). In this manner, the changes in PL  
11 spectra and PL decay time were investigated step by step. The PL intensity change after each  
12 step for untreated (w/o AS) and AS-treated (w/ AS) samples is given as a ratio in **Figure 2**.  
13 After the AS treatment, PL peak maximum increased 11-, 4- and 7-fold for Cu-poor, desired,  
14 and rich samples, respectively. However, the PL peak maximum decreased after slightly after  
15 CdS deposition for the Cu-poor and Cu-desired samples. We believe this is due to the fact  
16 that, during the chemical bath deposition, the CdS layer forms in a slightly different way on  
17 each sample as the formation of the buffer layer is impacted by changes on the sample surface  
18 and/or its composition. This could, then, lead to slight changes in the thickness of CdS, which  
19 can cause some absorption of the 532nm laser light of the PL setup. Nevertheless, when  
20 comparing the CdS covered samples with and without AS-treatment, it can be clearly seen  
21 that the PL intensity is higher for the samples with AS-treatment. Therefore, it can be said that  
22 AS-treatment has beneficial impact on CIGS surface and improves the quality of the interface  
23 between CIGS and CdS. **Figure 3a and b** show the changes in FWHM upon CdS deposition  
24 for untreated (w/o AS) and AS-treated (w/ AS) samples. Changes in the high and low energy  
25 peaks are shown for all 3 CGI ratios. The FWHM is determined by fitting the PL spectra  
26 using Gaussian peaks. Changes after AS treatment only (thus without CdS) are not shown

1 here because the FWHM decreases only minimally. In **Figure 3a**, the FWHM of the peak at  
2 high energy after CdS deposition is presented. As can be seen, the peak at high energy  
3 continuously gets sharper with increasing CGI ratio (light dashed line in Figure 3a), as we  
4 previously discussed in the context of Figure 1. This effect is further amplified by the AS  
5 treatment (dark dashed line in Figure 3a). The FWHM change of the low energy peak after  
6 CdS deposition is given in **Figure 3b**. Here, it is clearly visible that the peak gets broader with  
7 AS treatment. This could mean that the defect related peak is disappearing after surface  
8 treatment. These significant changes on high energy and low energy peaks could be explained  
9 by the fact that sulfur fills the copper vacancies and thus  $S_{Cu}$  forms during the surface  
10 treatment.<sup>[27,28]</sup> The improvements on the PL maximum and the FWHM of the high energy  
11 peak may be expected since it has been previously shown that CdS has a passivating effect on  
12 CIGS by substituting Cd into  $V_{Cu}$ .<sup>[22,29,30]</sup> As the PL maximum and FWHM further change  
13 upon AS, this passivation effect of CdS seems to be enhanced by the AS surface treatment.  
14 This enhancement could be related to the reduction of copper vacancies by sulfur substitution.  
15 Both effects due to the substitution of Cd and S then combine and generate a reduction in  
16 availability of copper vacancies. This reduces the overall concentration of  $(2V_{Cu}+In_{Cu})$  defects  
17 in the material, thereby reducing the defect related low energy peak in the PL response.  
18 Another option, in the case of the Cu-rich samples, is the removal of any possible  $Cu_{2-x}Se$   
19 secondary phase.  
20 The PL decay time of the samples for bare CIGS, after AS-treatment and after CdS deposition  
21 is given for all 3 CGI ratios in **Figure 4 (a-c)**. In PL decay graph for each ratio, only one  
22 curve of the bare CIGS was given for own CGI ratio, since all bare samples have a similar  
23 low PL decay time ( $\sim 1$ ns) independent of CGI ratio. The PL decay time improved  
24 significantly after AS treatment for Cu-poor and Cu-desired samples, however, for the Cu-  
25 rich sample, clear improvement on the PL decay time could not be observed. Moreover, the  
26 PL decay time of samples without AS treatment was improved after CdS deposition (w/o AS



1 CIGS+CdS). This CdS related improvement was further enhanced after AS treatment for all  
 2 samples, but the most significant change was observed for the Cu-poor and Cu-desired  
 3 samples (w/ AS CIGS+CdS). Thus, it appears that the passivation effect of AS is more  
 4 effective on Cu-poor and Cu-desired absorbers. This can be explained by the filling of  $V_{Cu}$   
 5 with sulfur, and thus reduction of the complex defect ( $2V_{Cu}+In_{Cu}$ ). For Cu-rich sample,  
 6 alongside the possible reduction of the concentration of ( $2V_{Cu}+In_{Cu}$ ), the  $Cu_{2-x}Se$  secondary  
 7 phases could be removed as well with AS, since AS is a known etchant for this secondary  
 8 phase.<sup>[9]</sup>

### 10 2.3. The effect of ammonium sulfide (AS) surface treatment on device performance

11 In this section, the samples that we used in the PL study were processed into solar cells. An  
 12 improving trend with AS-treatment similar to the one detected in the PL and TRPL  
 13 measurements was also observed in current-voltage (I-V) measurements. The solar cell  
 14 parameters are given **Figure 5**. In our measurements, the  $V_{oc}$  improved for the Cu-poor and  
 15 Cu-desired samples, but decreased for the Cu-rich sample. The FF improved for the Cu-  
 16 desired and Cu-rich samples, but decreased slightly for the Cu-poor sample, while the current  
 17 increased or remained constant. When the surface recombination decreases following  
 18 chemical surface passivation, open circuit voltage ( $V_{oc}$ ) and fill factor (FF) are expected to  
 19 improve.<sup>[31]</sup> An increase in  $V_{oc}$  can be estimated from the PL yield, by transforming the  
 20 Lasher-Stren-Wurfel equation into: <sup>[32]</sup>

$$21 \quad \Delta\mu_{AS-ref} = kT \ln\left(\frac{I_{AS}}{I_{ref}}\right) \quad (2)$$

22  $I_{AS}$  is PL peak maximum of the high energy peak of the AS-treated samples and  $I_{ref}$  is the PL  
 23 peak maximum of the high energy peak of the reference, i.e. the untreated sample. Both  
 24 intensities are after CdS deposition.  $\Delta\mu$  is the quasi Fermi level spitting, which is an  
 25 equivalent measure for the maximum  $V_{oc}$ . Thus, changes in  $\Delta\mu$  can be directly related to

1 changes in  $V_{oc}$ . According to equation 2, the expected improvement in  $V_{oc}$  was 15, 20 and 35  
2 mV for Cu-poor, Cu-desired and Cu-rich respectively. In the case of the Cu-poor and Cu-  
3 desired samples, we measured an improvement in the open circuit voltage after AS treatment  
4 of 12mV and 20mV, respectively. These values are in good agreement with the improvements  
5 predicted by equation 2. This leads us to conclude that surface treatment with AS has a similar  
6 effect to surface passivation in the case of the Cu-desired and Cu-poor samples. The predicted  
7  $V_{oc}$  improvement was not observed for the Cu-rich sample, since the  $V_{oc}$  for the AS treated  
8 sample is lower than for the untreated sample. This reduction of the  $V_{oc}$  could be related to the  
9 duration of the surface treatment. Buffiere et al. showed that for a CIGS sample with CGI:0.9  
10 one can observe a drop in  $V_{oc}$  if the sample is etched with AS for too long. Nevertheless, the  
11 performance of their solar cells was improved due to a gain in short circuit current.<sup>[9]</sup> This  
12 current gain was also observed for our Cu-rich sample. Thus, it can be said that the  
13 improvement in device performance is mostly related to removing possible  $Cu_{2-x}Se$  secondary  
14 phases. The EQE corrected power conversion efficiency of samples increased with AS  
15 treatment from 7.8% to 8%, from 5% to 6%, and from 6.6% to 8.2% for the Cu-poor, Cu-  
16 desired and Cu-rich champion cells, respectively. This improvement was either due to  
17 increased  $V_{oc}$  or  $J_{sc}$ . These results indicate that, during the AS-treatment, a combination of  
18 different effects takes place. It can be said that the observed improvements are either coming  
19 from the passivation of the surface or are possibly due to removal of secondary phases for the  
20 Cu-rich sample. Unfortunately, the device performance of our one-stage co-evaporated CIGS  
21 is still limited by other factors. Typically, the performance of this type of material is lower  
22 than for the more conventionally used 3-stage co-evaporated samples. This is mainly due to  
23 the fact that, in our samples there is no Ga-grading at front and back surface. Therefore, the  
24 interface recombination at both front and back interface is more critical and is one of the  
25 limiting factor for our device performance.<sup>[33]</sup> Also, our CIGS has relatively small grains  
26 (<100nm), and thus more grain boundaries.<sup>[34]</sup> The grain boundaries are generally accepted in

1 their role as recombination centers. The high concentration of them is, thus, another limiting  
2 factor for device performance. Due to these limiting factors in the bulk and the back interface,  
3 the significant improvements in PL cannot be reflected 'as is' to the performance of the  
4 devices, since AS-treatment is only affecting the CdS/CIGS front surface. Nevertheless, the  
5 AS treatment shows definite improvements for all studied CGI ratios. Therefore, it can be said  
6 that AS surface treatment is an easy and promising way to improve the buffer/CIGS interface.

### 7 8 **3. Conclusion**

9 In this study, firstly, we investigated the effect of the CGI ratio on CIGS thin films. The  
10 photoluminescence spectra revealed two peaks which behaved differently depending on the  
11 CGI ratio. A low energy peak, related to the  $(2V_{Cu}+In_{Cu})$  transition, is decreasing in intensity  
12 with increasing CGI ratio and a high energy peak, related to the band to band transition,  
13 becomes sharper. One possible explanation can be a lowering of the amount of Cu vacancies  
14 with increasing Cu-content. The reduced availability of Cu vacancies reduced the intensity of  
15 the low energy peak by limiting the formation of the  $(2V_{Cu}+In_{Cu})$  defect complex and sharpens  
16 the high energy peak (band-to-band transition) by reducing band fluctuations.

17 Then, the effect of ammonia sulfide (AS) treatment on these samples with different CGI ratio  
18 was investigated. The PL intensity and PL decay time are improved after AS-treatment and this  
19 improvement is maintained after the CdS deposition. We believe this enhancement could be  
20 due, once more, to the reduction in the density of Cu vacancies. This reduction takes place  
21 through filling of these vacancies with a sulfur atom during the AS-treatment. In addition, for  
22 the Cu-rich sample, the removal of  $Cu_{2-x}Se$  secondary phase is possibly a cause for the observed  
23 improvements.

24 Measuring the I-V characteristic of the samples processed into solar cells, the performance was  
25 shown to improve with AS-treatment. The improvement of the solar cell parameters such as  
26  $V_{oc}$  and FF indicates that the AS surface treatment has an effect comparable to surface

1 passivation on the Cu-poor and Cu-desired samples. However, for the Cu-rich sample, the  
2 improved performance is mostly due to an increased  $J_{sc}$  which can be due to the removal of the  
3 secondary phases.

4 In this paper, we showed that when the AS-treatment is applied to the surface of the CIGS  
5 absorber before deposition of the CdS layer, the PL decay time and the performance of the  
6 devices are enhanced for all CGI ratios. An absolute improvement of up to 1.16% was observed  
7 in the solar cell performance. Combining the AS treatment with a passivation layer may  
8 improve the performance of solar cells even further. Our results show that the AS surface  
9 treatment could be an effective way to passivate the front surface by reducing interface defects  
10 and removing the secondary phases, thus improving the interface between CIGS and CdS buffer  
11 layer. Further research is currently being focused on explaining the exact impact of the  
12 treatments and different ways to passivate the other factors limiting the efficiency of our solar  
13 cells.

#### 14 **4. Experimental Section**

15 *CIGS absorber processing:* The CIGS is deposited on SLG/Si(O,N)/Mo/2nm NaF/ substrate by  
16 using a one-stage co-evaporation process. The evaporation rates of the all sources (Cu, In, Ga  
17 and Se) are kept constant during the absorber layer deposition until the thickness of 450-500nm  
18 and desired composition are obtained. Thanks to this process a flat and homogenous Ga profile  
19 is achieved in the CIGS layer.<sup>[32]</sup> Three sets with different Cu/(Ga+In) (CGI) ratio were created.  
20 Sets are named according to the CGI ratio; CGI is 0.72 for Cu-poor, Cu-desire CGI: 0.8 and  
21 Cu-rich CGI: 0.92. Each set contains two absorbers: i- standard process (bare CIGS - (w/o AS)  
22 CdS), ii- surface treatment process (bare CIGS - AS treatment - (w/ AS) CdS). The composition  
23 and thickness were measured with X-ray fluorescence (XRF) and an XRF map is generated for  
24 each sample.

25 *Characterization:* Photoluminescence (PL) and time-resolved PL (TRPL) measurements are  
26 performed with a Picoquant FluoTime 300 system with an excitation wavelength 532nm (25ps,

1 3MHz). PL and TRPL measurements are taken before and after AS surface cleaning, and after  
2 CdS deposition. With the help of the XRF map, PL and TRPL are taken at the same 3 points  
3 for bare CIGS samples (the first set), and 4 points for the samples that are used as solar cells  
4 (the second set). The performance of the solar cells is measured at room temperature by using  
5 a solar simulator equipped with AM1.5 filter and a Keithley 2401 sourcemeter.

6 *Ammonium Sulfide (AS) treatment:* The AS solution with 6-7.5% sulfur concentration is used  
7 for surface treatment. The CIGS samples are dipped into the AS solution for 5min and followed  
8 by 2 times 2min of rinsing in deionized water before being dried with a nitrogen gun.

9 *Solar Cell Processing:* After the AS treatment, a CdS buffer layer (30-40 nm) is deposited on  
10 reference and AS-treated samples by chemical bath deposition. The aqueous solution is  
11 prepared with a cadmium acetate dihydrate (2.7 mM), thiourea (95 mM), ammonia (2.2 M) at 65  
12 °C and the deposition takes place in approximately 13min. Solar cells are produced by  
13 sputtering an i-ZnO/Al:ZnO window layer and finished with Ni/Al/Ni grids.

14

## 15 **Acknowledgements**

16 This work received funding from the European Union's H2020 research and innovation  
17 program under grant agreement No. 715027.

18

19 Received: ((will be filled in by the editorial staff))

20 Revised: ((will be filled in by the editorial staff))

21 Published online: ((will be filled in by the editorial staff))

22

23

24

## 25 **References**

26 [1] M.A. Green, E.D. Dunlop, J. Hohl-Ebinger, M. Yoshita, N. Kopidakis, A.W.Y. Ho-  
27 Baillie, Prog. Photovoltaics Res. Appl. **2020**, 28, 3

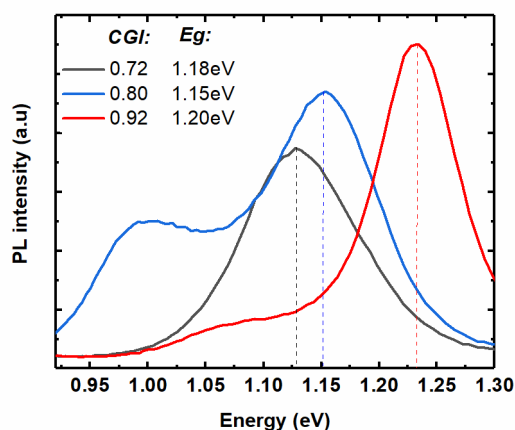
28 [2] T. Nakada, Electron. Mater. Lett. **2012**, 8, 179

29 [3] B. Vermang, J.T. Wätjen, V. Fjällström, F. Rostvall, M. Edoff, R. Kotipalli, F. Henry,

- 1 F. Denis, Prog. Photovoltaics Res. Appl. **2014**, 22, 1023
- 2 [4] G. Birant, J. de Wild, M. Meuris, J. Poortmans, B. Vermang, Appl. Sci. **2019**, 9, 677
- 3 [5] S. Garud, N. Gampa, T.G. Allen, R. Kotipalli, D. Flandre, M. Batuk, J. Hadermann, M.  
4 Meuris, J. Poortmans, A. Smets, B. Vermang, Phys. Status Solidi A. **2018**, 1700826, 1
- 5 [6] J. Löckinger, S. Nishiwaki, B. Bissig, G. Degutis, Y.E. Romanyuk, S. Buecheler, A.N.  
6 Tiwari, Sol. Energy Mater. Sol. Cells. **2019**, 195, 213
- 7 [7] Y. Hashimoto, N. Kohara, T. Negami, M. Nishitani, T. Wada, Jpn. J. Appl. Phys., **1996**  
8 35, 4760
- 9 [8] H. Marko, L. Arzel, A. Darga, N. Barreau, S. Noël, D. Mencaraglia, J. Kessler, Thin  
10 Solid Films. **2011**, 519, 7228
- 11 [9] M. Buffière, A.A. El Mel, N. Lenaers, G. Brammertz, A.E. Zaghi, M. Meuris, J.  
12 Poortmans, Adv. Energy Mater. **2015**, 5, 1
- 13 [10] B. Canava, J. Vigneron, A. Etcheberry, D. Guimard, J. Guillemoles, D. Lincot, Thin  
14 solid Films, **2002**, 403-404, 425
- 15 [11] J. Li, Y. Ma, G. Chen, J. Gong, X. Wang, Y. Kong, X. Ma, K. Wang, W. Li, C. Yang,  
16 X. Xiao, Sol. RRL. **2019**, 3, 1
- 17 [12] C.L. Perkins, F.S. Hasoon, H.A. Al-Thani, S.E. Asher, P. Sheldon, Conf. Rec. IEEE  
18 Photovolt. Spec. Conf. **2005**, 255
- 19 [13] T. Nakada, K. Matsumoto, M. Okumura, Conf. Rec. IEEE Photovolt. Spec. Conf.  
20 **2002**, 527
- 21 [14] W. Li, S.R. Cohen, D. Cahen, Sol. Energy Mater. Sol. Cells. **2014**, 120, 500
- 22 [15] W.N. Shafarman, S. Siebentritt, L. Stolt, *Handbook of Photovoltaic Science and*  
23 *Engineering*, Second Edi, John Wiley & Sons, 2011.
- 24 [16] D.G. Buldu, J. De Wild, T. Kohl, G. Birant, G. Brammertz, J. Poortmans, B. Vermang,  
25 IEEE 46th Photovolt. Spec. Conf. ,Chicago, IL, USA, **2019**
- 26 [17] D. Lee, J.Y. Yang, Y.S. Kim, C.B. Mo, S. Park, B.J. Kim, D. Kim, J. Nam, Y. Kang,

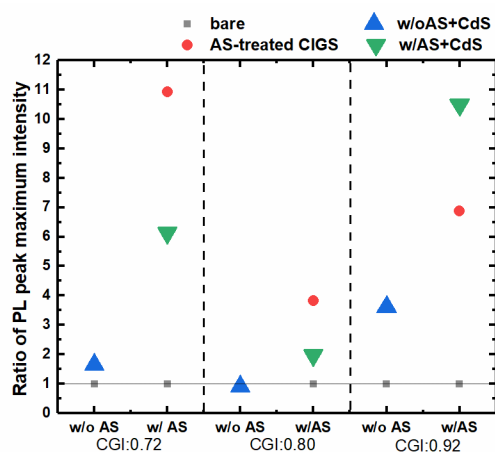
- 1 Sol. Energy Mater. Sol. Cells. **2016**, 149, 195
- 2 [18] A. Hultqvist, J. V Li, D. Kuciauskas, P. Dippo, M.A. Contreras, D.H. Levi, F. Stacey, ,  
3 Appl. Phys. Lett. **2015**, 107, 033906
- 4 [19] S.B. Zhang, S.H. Wei, A. Zunger, Phys. Rev. Lett. **1997**, 78, 4059
- 5 [20] S.B. Zhang, S. Wei, A. Zunger, Phys. Rev. B. **1998**, 57, 9642
- 6 [21] M.H. Wolter, Optical Investigation of Voltage Losses in High-Efficiency Cu(In,Ga)Se<sub>2</sub>  
7 Thin-Film Solar Cells, Universite Du Luxembuorg, 2019.
- 8 [22] S. Shirakata, K. Ohkubo, Y. Ishii, T. Nakada, Sol. Energy Mater. Sol. Cells. **2009**, 93,  
9 988
- 10 [23] J. Parravicini, M. Acciarri, M. Murabito, A. Le Donne, A. Gasparotto, S. Binetti, Appl.  
11 Opt. **2018**, 57, 1849
- 12 [24] J.H. Schon, C. Kloc, E. Bucher, Thin Solid Films. **2000**, 362, 411
- 13 [25] J. Yang, H.W. Du, Y. Li, M. Gao, Y.Z. Wan, F. Xu, Z.Q. Ma, AIP Adv. **2016**, 6,  
14 085215
- 15 [26] S. Ishizuka, A. Yamada, M.M. Islam, H. Shibata, P. Fons, T. Sakurai, K. Akimoto, S.  
16 Niki, J. Appl. Phys. **2009**, 106, 034908
- 17 [27] X. Liu, Z. Liu, F. Meng, M. Sugiyama, Sol. Energy Mater. Sol. Cells. **2014**, 124, 227
- 18 [28] Y. Nam, J. Yoo, S.K. Chang, J.H. Wi, W.J. Lee, D.H. Cho, Y.D. Chung, J. Lumin.  
19 **2017**, 188, 595
- 20 [29] S.-H. Chen, W.-T. Lin, S.-H. Chan, S.-Z. Tseng, C.-C. Kuo, S.-C. Hu, W.-H. Peng, Y.-  
21 T. Lu, ECS J. Solid State Sci. Technol. **2015**, 4, 347
- 22 [30] S. Shirakata, T. Nakada, Phys. Status Solid C. **2009**, 1062, 1059
- 23 [31] G. Sozzi, S. Di Napoli, R. Menozzi, B. Bissig, S. Buecheler, A.N. Tiwari, Sol. Energy  
24 Mater. Sol. Cells. **2017**, 165, 94
- 25 [32] J. De Wild, D.G. Buldu, T. Schnabel, M. Simor, T. Kohl, G. Birant, G. Brammertz, M.  
26 Meuris, J. Poortmans, B. Vermang, ACS Appl. Energy Mater. **2019**, 2, 6102

- 1 [33] Y. Kong, J. Li, Z. Ma, Z. Chi, X. Xiao, J. Mater. Chem. A. **2020**, 8, 9760
- 2 [34] T. Kohl, N.A. Rivas, J. de Wild, D.G. Buldu, G. Birant, G. Brammertz, M. Meuris,
- 3 F.U. Renner, J. Poortmans, B. Vermang, ACS Appl. Energy Mater. **2020**, 3, 5120
- 4



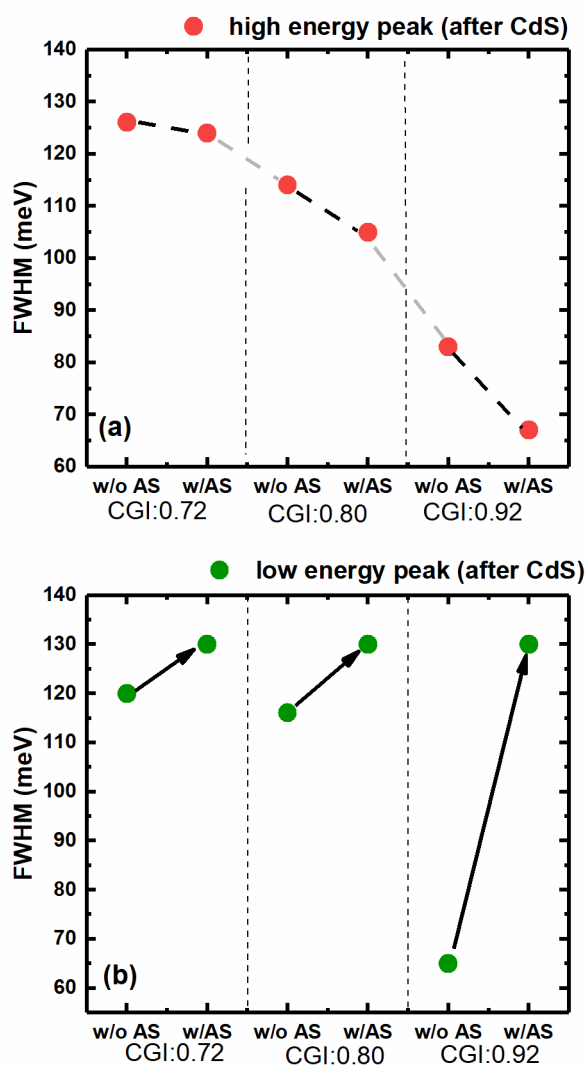
5  
6 **Figure 1.** PL spectra of the bare CIGS samples with different Cu/(Ga+In) ratios and their calculated  
7 band gap energies ( $E_g$ ). The peak maximum is represented with a dashed line to highlight the  
8 difference with the calculated band gap. As the CGI ratio increases, the high energy peak gets sharper  
9 and more intense.

10

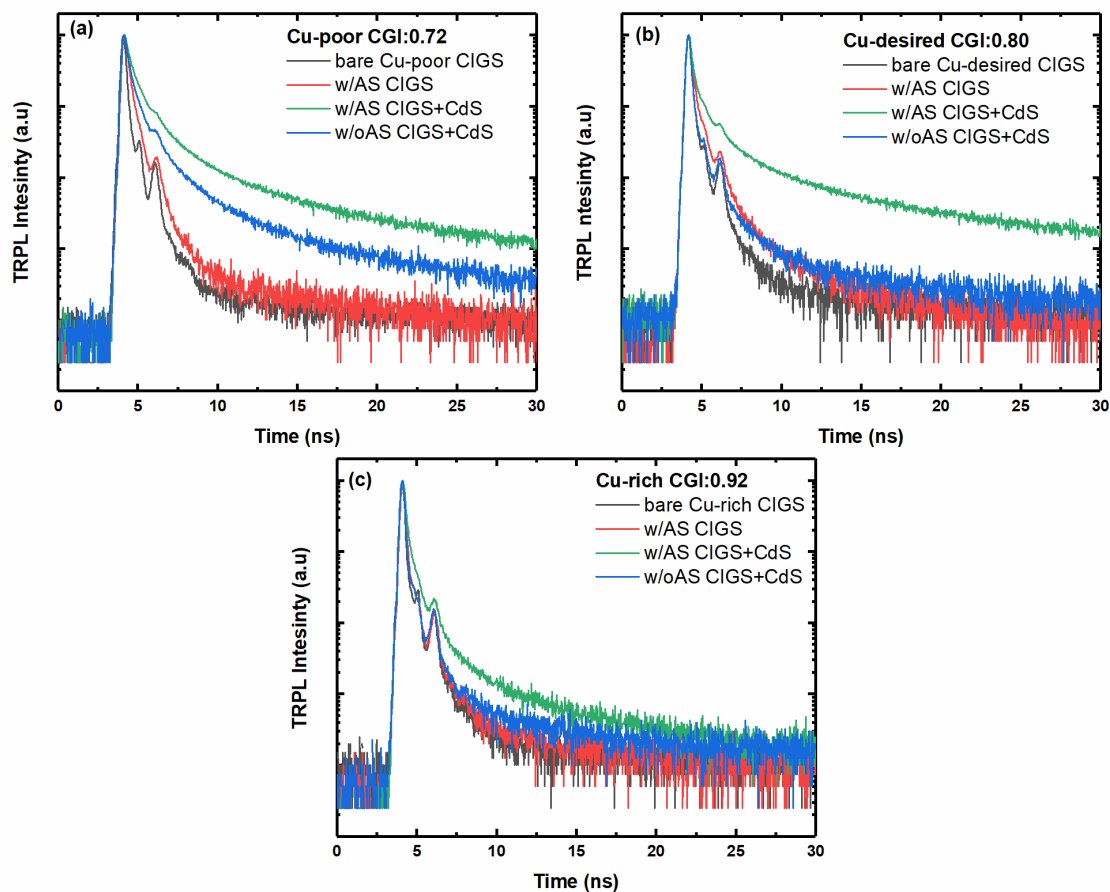


11  
12 **Figure 2.** The change in PL intensity of the peak at high energy as compared to the bare absorber is  
13 shown as a ratio for each sample (w/o AS and w/ AS) for each CGI ratio. The bare absorbers are  
14 represented using squares. The ratio between bare and after AS-treatment is represented with dots.  
15 The ratios between bare and after CdS deposition are represented using blue triangles for the  
16 untreated (w/o AS) and green triangles for the AS treated (w/ AS) samples.

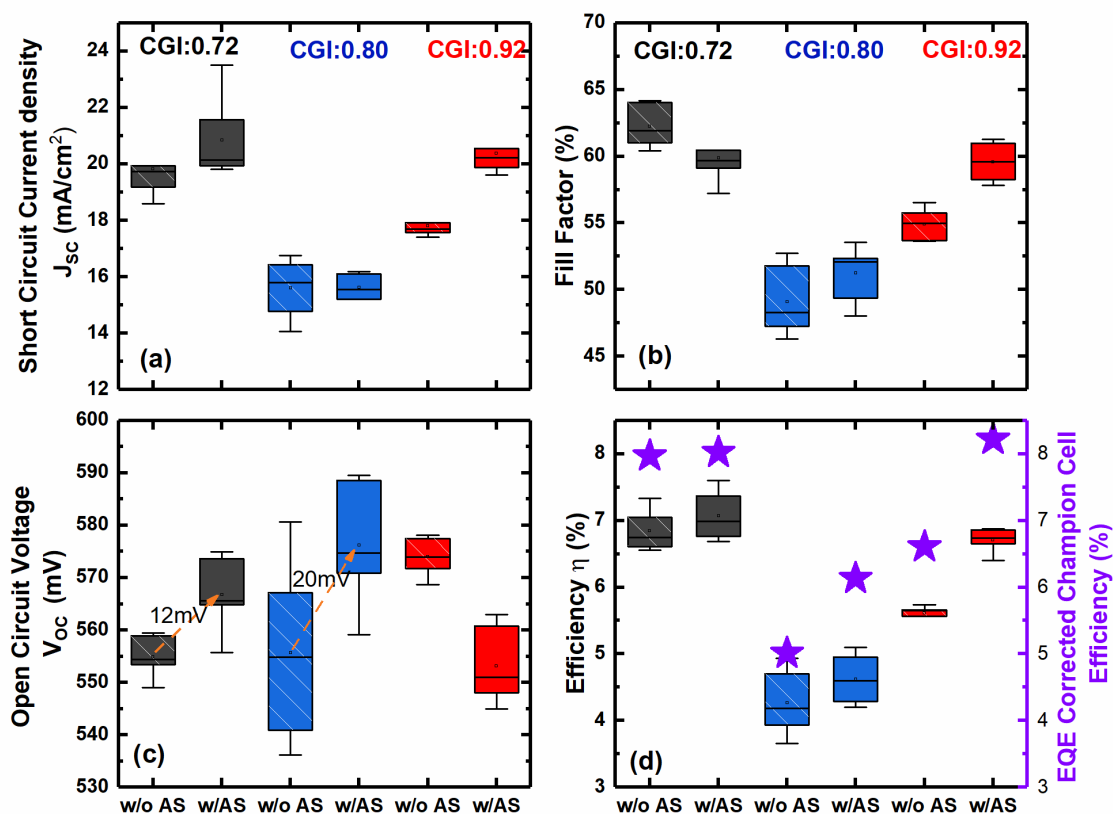




1  
2 **Figure 3.** (a) The change in FWHM of the high energy peak after CdS deposition for each sample (w/o  
3 AS and w/ AS) for each CGI ratio. The dashed line is a guide to the eye following the evolution of the  
4 FWHM of the high energy peak (dots), and shows that the peak is consistently getting narrower after  
5 AS treatment when compared to the untreated samples (w/o AS). (b) The trend in FWHM of the low  
6 energy peak (green dots) shows that it is broadening with AS treatment.



1  
 2 **Figure 4.** The PL decay lifetime for bare CIGS, after AS-treatment (w/ AS CIGS) and after CdS for  
 3 both untreated (w/o AS) and AS-treated (w/ AS) for (a) Cu-poor (b) Cu-desired and (c) Cu-rich  
 4 samples. The black continuous line stands for the bare CIGS absorber, the CIGS absorber after AS-  
 5 treatment is red. The green line is after CdS deposition for AS-treated sample and the blue one is for  
 6 the CdS deposited sample w/o AS-treatment. In all cases, the PL decay time improves after the  
 7 deposition of the CdS layer. This effect is enhanced if CdS is deposited after treating the sample with  
 8 AS.



1  
2 **Figure 5.** Electrical parameters of the untreated (w/o AS) and the AS-treated (w/AS) samples for each  
3 CGI ratio. (a)  $J_{sc}$ , (b) fill factor (c)  $V_{oc}$ . The arrows indicate the gain in  $V_{oc}$  after AS-treated samples.  
4 (d) Efficiency. The EQE corrected best cell efficiencies (star) for each CGI ratio.

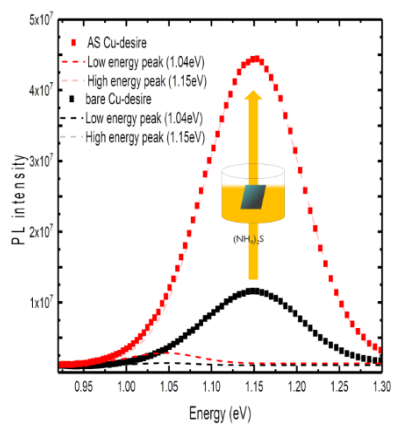
5 This work shows that ammonium sulfide surface treatment plays a key role to improve the  
6 buffer layer/CIGS interface. The exact impact of the surface treatment could be different  
7 depending on the Cu/(Ga+In) ratio. However, independent of this ratio, ammonium sulfide  
8 surface treatment has a net positive effect on the performance of all studied samples.  
9

10 **Keyword** surface treatment, Cu(In,Ga)Se<sub>2</sub>, CGI ratio, thin-film photovoltaics,  
11 photoluminescence

12  
13 Jessica de Wild, Thierry Kohl, Guy Brammertz, Gizem Birant, Marc Meuris, Jef Poortmans,  
14 Bart Vermang, Dilara Gokcen Buldu\*

15  
16 **Study of ammonia sulfide surface treatment for ultra-thin Cu(In,Ga)Se<sub>2</sub> with different  
17 Cu/(Ga+In) ratios**

18  
19 **ToC figure ((Please choose one size: 55 mm broad × 50 mm high or 110 mm broad × 20  
20 mm high. Please do not use any other dimensions))**



1  
2  
3  
4

Copyright WILEY-VCH Verlag GmbH & Co. KGaA, 69469 Weinheim, Germany, 2018.